Journal oejiang University SCIENCE A
ISSN 1673-565X (Print); ISSN 1862-1775 (Online)
www.zju.edu.cn/jzus; www.springerlink.com
E-mail: jzus@zju.edu.cn

# Preparation of nano-$TiO_2$ photocatalysts and their decomposition activity in phenol-contaminated water

Xiao-yuan JIANG†, Feng DU, Chun-xia GUO, Qiong YANG, Xiao-ming ZHENG

(*Institute of Catalysis, Faculty of Science, Zhejiang University, Hangzhou 310028, China*)

†E-mail: xyjiang@mail.hz.zj.cn

Received Oct. 5, 2008; Revision accepted Jan. 21, 2009; Crosschecked July 7, 2009

**Abstract:** $TiO_2$ was prepared by the hydrolyzation method in $(NH_4)_2SO_4$-modified $TiCl_4$ solution, and $TiO_2$ photocatalysts were obtained by accelerating the precipitation of $TiO_2$ powder in a high-temperature water bath. The photocatalysts were characterized by Brunauer-Emmett-Teller (BET), X-ray diffraction (XRD), Raman spectrum and UV-Vis (Ultraviolet-Visible) spectrometry techniques, and the photocatalytic activity in phenol-contaminated water was investigated. The results showed that photocatalysts calcined at 400 °C had a specific surface area of 138.2 $m^2$/g and an average particle size of 9 nm, and a significant increase in thermal stability of anatase phase. At the calcination temperature of 700 °C, the crystal form of $TiO_2$ started to change into rutile (anatase: 97%, rutile: 3%). The activity of $TiO_2$ photocatalysts prepared with $(NH_4)_2SO_4$-modified $TiCl_4$ solution was markedly stronger than that without $(NH_4)_2SO_4$-modified $TiCl_4$ solution. Maximal photocatalytic activity was observed at the mole ratio of Ti:$(NH_4)_2SO_4$=1:2, the water-bath temperature of 90 °C and the calcination temperature of 700 °C.

**Key words:** Ammonium sulfate, Titanium dioxide, Photocatalysis reaction, Phenol-contaminated water
**doi:**10.1631/jzus.A0820687 **Document code:** A **CLC number:** R733.7

## INTRODUCTION

Zhang *et al.*(1999) and Gao and Zhang (2001) first reported that adding $(NH_4)_2SO_4$ into the procedure of preparing $TiO_2$ photocatalysts by $TiCl_4$ hydrolysis could produce nanometer-sized particles and improve the thermal stability of anatase phase. Under optimal conditions, the minimum average particle size of $TiO_2$ powder was 3.8 nm and its specific surface area was 290 $m^2$/g. Su *et al.*(2001) prepared $SO_4^{2-}/TiO_2$ solid super acidic photocatalysts using the impregnation method in 1 mol/L $H_2SO_4$ solution and found that surface modification of $SO_4^{2-}$ markedly improved the structure of $TiO_2$ photocatalysts. Compared with normal $TiO_2$, the $TiO_2$ of super acidic solid $SO_4^{2-}/TiO_2$ had the following characteristics: higher anatase content, smaller crystal grain, bigger specific surface area, more concentrated pore-size distribution, better photocatalytic activity and wet-repellent function. Colon *et al.*(2003; 2006) prepared powdery $TiO_2$ by the sol-gel method using $H_2SO_4$ solution impregnation, and observed that the photocatalysts still had high activity at the calcination temperature of >600 °C. This was probably because a small amount of $SO_4^{2-}$ adsorbed on the $TiO_2$ precursor greatly improved the thermal stability of anatase phase, and decomposed at >600 °C to produce a great number of O ions, which increased the oxygen-hole quantity of catalyst surface and led to form a Schottky potential hill on the catalyst surface. The increment of oxygen-hole quantity and the formation of a Schottky potential hill could prevent recombination of electron-hole pairs caused by the excitation of light source, and therefore improved the light efficiency and activity of photocatalysts.

In this study, $TiO_2$ photocatalysts were prepared with an improved hydrolyzation method using high-temperature water bath to accelerate the precipitation of powdery $TiO_2$ and adding $(NH_4)_2SO_4$ to $TiCl_4$ aqueous solution. The obtained photocatalysts had big specific surface areas, a small average particle

size and high thermal stability. After calcination at 400 °C, the photocatalysts still had a specific surface area of 138.2 $m^2/g$ and an average particle size of 9 nm, and the thermal stability temperature of anatase phase at about 700 °C.

## MATERIALS AND METHODS

### Catalyst preparation

A 600 ml beaker with 90 ml deionized water was put in an ice-water bath, and 10 ml of $TiCl_4$ solution were slowly dripped and agitated in the beaker (0.9 mol/L). 24 g of $(NH_4)_2SO_4$ crystal were dissolved in 90 ml deionized water (0.18 mol/L) in another 600 ml beaker, and then slowly dripped into the $TiCl_4$ solution in an ice-water bath. The mixture was put in a water bath at 90 °C, and added with 1:1 (v/v) ammonia dropwise until pH=7 (2.5 ml/min). After aging for 1 h, the mixture was cooled to room temperature (RT) in air, shrinked filter, cleansed with deionized water to remove $Cl^-$, washed with alcohol two times and then dried at 110 °C for 12 h to produce powdery $TiO_2$. The powdery $TiO_2$ was placed into a muffle furnace and calcined at the temperatures of 400, 500, 600, 700 and 800 °C, ramped at a linear heating rate of 3 °C/min for 2 h. The $TiO_2$ photocatalysts were named TS(1:2)400, TS(1:2)500, TS(1:2)600, TS(1:2)700, TS(1:2)800 respectively, with T as $TiO_2$, S as improved $(NH_4)_2SO_4$, 1:*x* as the mole ratio of $Ti:SO_4^{2-}$, and 400 as the calcination temperature of 400 °C, and so on.

### Catalytic properties

Specific surface areas of catalysts were measured by the Brunauer-Emmett-Teller (BET) method based on $N_2$ adsorption at the liquid-nitrogen temperature using a Coulter OMNISORP-100 Instrument (Coulter Company, USA). Catalysts were degassed at 200 °C in vacuum ($1\times10^{-5}$ Pa) for 2 h.

Thermogravimetric and Differential Thermal Analysis (TG-DTA) spectra were measured using a PE-TGA7 thermogravimetric analyzer (Perkin Elmer Company) and a DTA/9050311 high temperature differential analyzer. 10 mg of fresh catalysts were taken and measured in air, and then treated in 150 ml/min of dry pure $N_2$ with temperatures ramped at a linear heating rate of 10 °C/min from 100 to 900 °C.

X-ray diffraction (XRD) data were obtained by a horizontal Rigaku B/Max IIIB powder diffractometer with the $CuK_\alpha$ radiation of a Ni filter and a 40 kV×30 mA power (D8Advance of Bruker, German). The diffraction angle was $2\theta$ (°), and the source of wavelength was $CuK_\alpha$=0.154 nm.

Ultraviolet-Visible (UV-Vis) spectra were measured using (UV-240, Shimadzu, Japan) (attached diffuse reflection determination device/accumulation points ball) and $BaSO_4$ standard reference powder. A certain amount of powdery $BaSO_4$ was placed in the sample cell and then flattened by an organic glass bar. $BaSO_4$ standard white boards were inserted into the sides of sample and reference beams in the accumulation points ball respectively, and then the background was adjusted. The particle size of the solid catalyst was 80 meshes, dried at 120 °C for 2 h, and then put into a desiccator. A certain amount of the powdery catalyst was placed in the sample cell and flattened by the organic glass bar, then inserted into one side of the sample beam in the accumulation points ball. The scanning scale of absorption spectrum was 190~800 nm using a $BaSO_4$ standard white board as reference.

Raman spectra were measured using a LabRaman HR 800 (Jobin Yvon Company, France) focusing micro Raman spectrograph, with a scanning width at 50~1000 $cm^{-1}$ and a light wavelength at 514 nm using $Ar^+$ ion laser as the excited light source. Facula size was 250 μm with lens size of 50 mm×10.50 mm and a power of 13 mW and spectrum resolution ratios of 1 $cm^{-1}$. The sample was put in a smooth glass sheet and then flattened.

### Measurements of catalytic activity

Catalytic activity was measured using phenol-contaminated water as the target degradation molecule. The initial concentration and volume of aqueous phenol solution were $C_0$ and 100 ml. Light source was a 300 W high-voltage mercury lamp with a wavelength of 365 nm. Catalysts and target molecules were mixed through addition and agitation. Reaction efficiency was estimated according to the concentrations of remnant phenol, while the concentrations of aqueous phenol solution in the reactor were determined every 30 min. After its centrifuge at 4500 r/min for 10 min, absorbance of the solution at 510 nm was measured by 722-spectrophotometry. Remnant concentration of phenol was derived corresponding to the

standard curve. Remanent volume of the solution was calculated using the formula $C/C_0$ (if there was no specific explanation, the initial concentration of aqueous phenol solution was 10 mg/L; when 2 g catalysts were used, the volume of phenol solution was 100 ml).

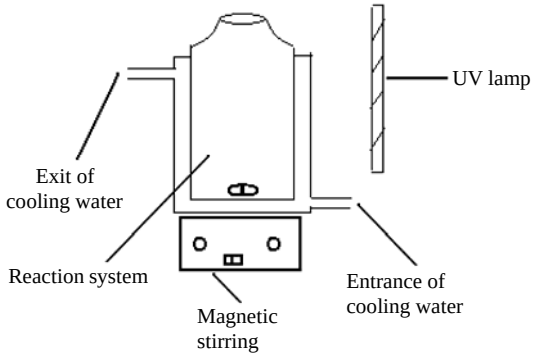


**Fig.1 Sketch map of the equipment for catalyst reaction**

## RESULTS

### Pore size distribution and adsorption-desorption isotherm of $TiO_2$

When $TiO_2$ photocatalysts were prepared without modified $(NH_4)_2SO_4$ solution in the water bath at 90 °C, the ring-opening area decreased with the increasing calcination temperature from 400 to 700 °C (Fig.2a). At the calcination temperature of 700 °C, the pore size distribution was mostly at 19 nm and had a small peak at <10 nm. When being calcined at 400 °C, the pore-size distribution was mainly at 14 nm (Fig.2b).

The adsorption-desorption isotherms and pore-size distribution curves of TS(1:2)400 and TS(1:2)700 in the water bath at 90 °C are shown in Figs.3a and 3b. The ring-opening area decreased with the increasing calcination temperature (Fig.3a). At the calcination temperature of 400 °C the pore-size distribution was mainly at 6 nm, whereas at that of 700 °C the pore-size distribution was mainly at 17 nm (Fig.3b).

As shown in Figs.2 and 3, after calcination at 400 °C, $TiO_2$ photocatalysts with $(NH_4)_2SO_4$ modification had a pore size of 6 nm and a specific surface area of 136.2 $m^2/g$, compared with 14 nm and 108.2 $m^2/g$ of those without $(NH_4)_2SO_4$ modification. In contrast, after calcination at 700 °C, the pore size of $TiO_2$ photocatalysts (17 nm) with $(NH_4)_2SO_4$

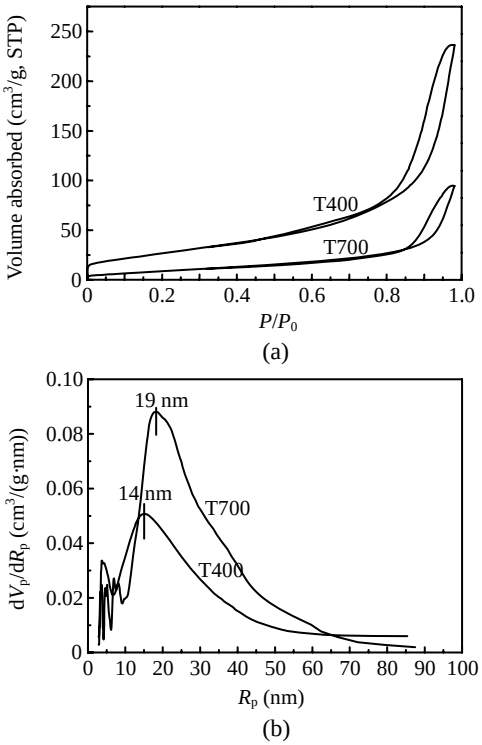


**Fig.2 Pore size distribution pattern (a) and adsorption-desorption isotherm (b) of T400 and T700 catalysts.**
STP: standard temperature and pressure; $R_p$: pore radius; $p$: pressure of adsorption balance; $p_0$: saturation vapor pressure

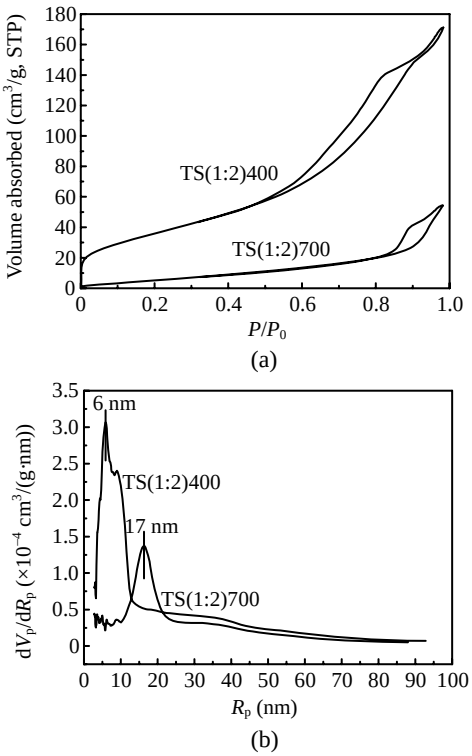


**Fig.3 Pore size distribution (a) and adsorption-desorption isotherm (b) of TS(1:2)400 and TS(1:2)700 catalysts**

modification was only slightly smaller than that of $TiO_2$ photocatalysts (19 nm) without $(NH_4)_2SO_4$ modification. Namely, $(NH_4)_2SO_4$ modification made the pore size of $TiO_2$ smaller and pore-size distribution more centralized. It also proved that the particles of $TiO_2$ photocatalysts prepared by $(NH_4)_2SO_4$ modification were more homogeneous.

## TG-DTA curve

The TG-DTA curves of $TiO_2$ photocatalysts with $(NH_4)_2SO_4$ modification in the water bath at 90 °C had two weight-lose steps (Fig.4a): one step at <400 °C likely due to volatilization of $H_2O$ and $C_2H_5OH$, and the other step at about 700 °C likely as a result of decomposition of absorbed $SO_4^{2-}$. By comparison, $TiO_2$ photocatalysts without $(NH_4)_2SO_4$ modification had only one weight-lose step at <400 °C (Fig.4b).

The TG curves in Figs.4a and 4b proved the existence of $(NH_4)_2SO_4$. In addition, an absorption heat peak in the DTA curve at 700~800 °C may indicate that $(NH_4)_2SO_4$ modification delayed the transformation of $TiO_2$ phase and increased the thermal stability of $TiO_2$.

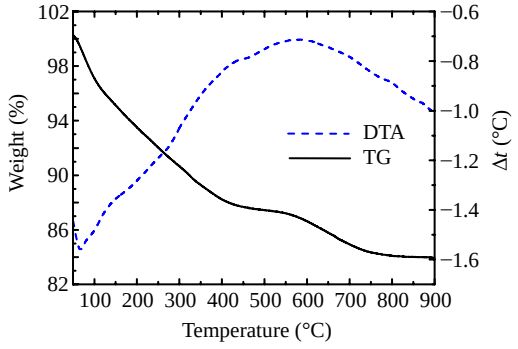


(a)

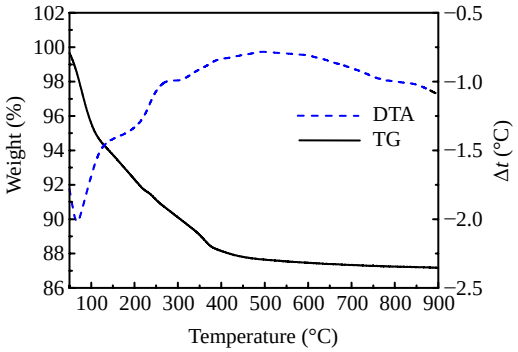


(b)

**Fig.4 TG-DTA pattern of (a) TS and (b) $TiO_2$**

## XRD diffraction

The $(NH_4)_2SO_4$ modification effectively suppressed crystal transformation of $TiO_2$ anatase to rutile (Fig.5). When being calcined at 700 °C, the main crystal form of $TiO_2$ was anatase (anatase: 97%, rutile: 3%). The XRD diffraction peak of $TiO_2$ calcined at 400 °C was diffusive, indicating that crystal $TiO_2$ was not fully formed at this temperature. At the calcination temperatures of 500 and 600 °C, the crystal form of $TiO_2$ was pure anatase. Although crystal $TiO_2$ was anatase 97% and rutile 3% at the calcination temperature of 700 °C, the diffraction peak of anatase became very small and the quantity of rutile increased significantly at the calcination temperature of 800 °C.

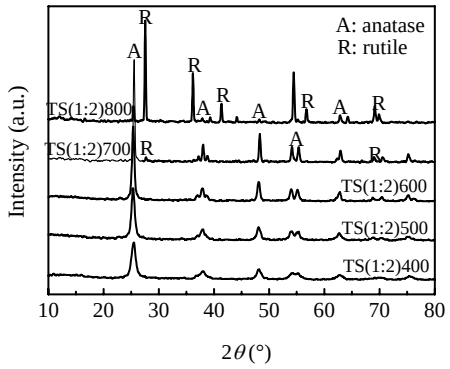


**Fig.5 XRD pattern of catalysts calcined at different temperatures**

After calcination at 700 °C, plenty of rutile occurred (about 60%) under $TiO_2$ without $(NH_4)_2SO_4$ modification, compared to mainly anatase under $TiO_2$ with $(NH_4)_2SO_4$ modification (Fig.6). Colon *et al.*(2006) examined that this was probably because the absorbed $SO_4^{2-}$ in the $TiO_2$ precipitation process increased the existing temperature of anatase, which was also shown by the TG-DTA data.

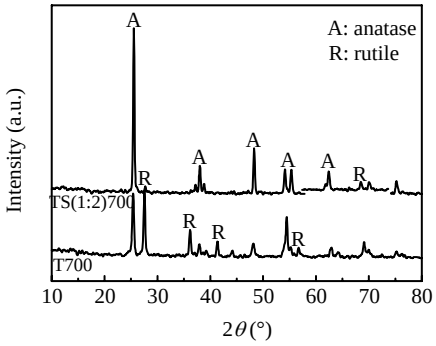


**Fig.6 XRD pattern of TS(1:2)700 and T700 catalysts**

The crystal forms of $TiO_2$ prepared at different water-bath temperatures were very similar (Fig.7), indicating that temperature had little effect on the formation of crystal $TiO_2$.

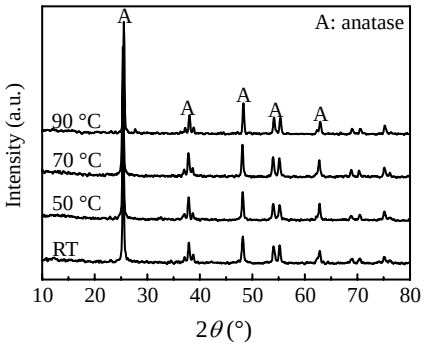


**Fig.7 XRD pattern of catalysts prepared at different water bath temperatures**

## Specific surface area and average particle size of $TiO_2$

Table 1 shows the data of BET, anatase content and average particle size of TS(1:2) catalysts calcined at different temperatures. The average particle size was calculated using the Warren-Averbach equation by Colon *et al.*(2003): $D=\lambda\times(180/\pi)\cos(\theta L)$ (where $L$ is the peak width of characteristic peak, $\lambda$ is 0.154 nm of X-ray wavelength, $\theta$ is the angle of diffraction). The effect of calcination temperature on the specific surface area and average particle size of photocatalysts TS(1:2) was very big (Table 1). The specific surface area of $TiO_2$ photocatalysts decreased sharply with the increasing calcination temperature: 136.2 $m^2/g$ at 400 °C, 83.8 $m^2/g$ at 500 °C, 46.5 $m^2/g$ at 600 °C, 28.2 $m^2/g$ at 700 °C, and only 18.1 $m^2/g$ at 800 °C. However, the average particle size of $TiO_2$ photocatalysts increased with the increasing calcination temperature: 9 nm at 400 °C, 13 nm at 500 °C, 16 nm at 600 °C, and 20 nm at 700 °C. The factor of affecting anatase content was calcination temperature: partial crystal formation at 400 °C, 100% formation of anatase at 500 °C and 600 °C, little transformation of anatase to rutile (3%) at 700 °C and a dramatic transformation of $TiO_2$ photocatalysts to rutile (70%) at 800 °C.

The effects of a homeothermic water bath and a 50 °C water bath on catalysts were small, but increasing the water bath temperature to 70 °C had a large effect on BET and the average particle size of $TiO_2$ photocatalysts (Table 2). At the water-bath temperature of 90 °C the difference in average particle size was 4~5 nm, probably because high temperatures accelerated the gathering of colloids. Ye (2006) examined the aggregation of colloid particles under given conditions is called gathering phenomenon. There are several factors that cause the gathering of colloid (i.e., conditions of destroying colloid stability), such as increasing the temperature, adding an electrolyte, adding a sol of opposite charge, optical effect and long-time dialysis. Increasing temperature may weaken the adsorption of colloidal particles to ions, destroy hydration shell of colloid, fasten colloidal movement and increase the chances of colliding and thus gathering between colloidal particles. Zhang *et al.*(2000) explained that there were three steps about $TiCl_4$ hydrolyzation:

$$TiCl_4+H_2O=TiOH^{3+}+H^++4Cl^-, \quad (1)$$

$$TiOH^{3+}=TiO^{2+}+H^+, \quad (2)$$

$$TiO^{2+}+H_2O=TiO_2+2H^+, \quad (3)$$

Eqs.(2) and (3) were the endothermic reactions, which explained the acceleration in precipitation of $TiO_2$ colloid to prevent from the creation of colloidal liquid and the gathering of $TiO_2$ with increasing water-bath temperatures, and as a consequence, fine powdery $TiO_2$ was obtained.

**Table 1 Data of BET, anatase content and average particle size of TS(1:2) catalysts calcined at different temperatures**

| Sample | Surface area ($m^2/g$) | Anatase (%) | Particle size (nm) |
|---|---|---|---|
| TS(1:2)400 | 136.2 | – | 9 |
| TS(1:2)500 | 83.8 | 100 | 13 |
| TS(1:2)600 | 46.5 | 100 | 16 |
| TS(1:2)700 | 28.2 | 97 | 20 |
| TS(1:2)800 | 18.1 | 30 | – |

**Table 2 Data of BET and average particle size of TS(1:2) catalysts prepared at different water bath temperatures**

| Sample | Surface area ($m^2/g$) | Particle size (nm) |
|---|---|---|
| RT-TS(1:2)700 | 23.4 | 24 |
| 50-TS(1:2)700 | 22.9 | 25 |
| 70-TS(1:2)700 | 26.2 | 23 |
| TS(1:2)700 | 28.2 | 20 |

**UV-Vis spectrum**

Fig.8 shows the UV-Vis absorption spectra of T400, TS(1:2)400, TS(1:2)700, TS(1:2)800 and P25 (gas-method $TiO_2$ produced by German Degussa Company) $TiO_2$ photocatalysts. Compared with P25 photocatalysts, the absorption limit of T400 occurred with a blue-shift but TS(1:2)400 and TS(1:2)700 with a bathochromic-shift. The degree of bathochromic-shift was TS(1:2)700>TS(1:2)400, and reached maximum by TS(1:2)800 that contained >70% of rutile. It is known that reaction energy mainly comes from light sources in photocatalysis reaction (Mei and Zhong, 2004). The absorption limit of $TiO_2$ photocatalysts occurred with a bathochromic-shift, indicating that its extinction ability and light-use efficiency were in favor of photoexcitation to increase the number of electron holes and thus the activity of $TiO_2$ photocatalysts. Because the energy difference of rutile was narrower than that of anatase (Han *et al.*, 2003), the bathochromic-shift degree of TS(1:2)800 that contained 70% rutile was the maximum.

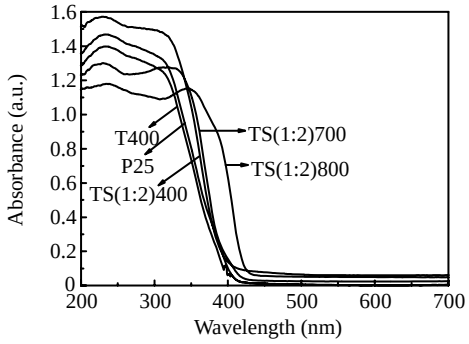


**Fig.8 UV-Vis diffuse reflectance spectroscopy of catalysts**

**Raman spectrum**

When the calcination temperature was below 700 °C, there were four peaks (161, 398, 518 and 637 $cm^{-1}$) in the Raman spectroscopy of TS(1:2) catalysts, but the shift peaks of TS(1:2)800 showed saltation at 250, 446 and 610 $cm^{-1}$ (Fig.9). According to Alemany *et al.*(2000), Raman shifts at 161, 398, 518 and 637 $cm^{-1}$ were the typical peaks of anatase, whereas the shift peaks at 250, 446 and 610 $cm^{-1}$ were the typical peaks of rutile. Therefore, when $TiO_2$ photocatalysts were calcined at 700 °C $TiO_2$ mainly existed as anatase; but with calcination at 800 °C rutile occurred markedly. $TiO_2$ photocatalysts calcined at 700 °C began to have crystal transformation, based on the XRD results. In addition, there is a weak characteristic peak of S—O band in 780~800 $cm^{-1}$ (Jung and Grange 2000), indicating that the $SO_4^{2-}$ content of $TiO_2$ photocatalysts prepared was very low and had formed $SO_4^{2-}/TiO_2$ solid super acid (Su *et al.*, 2001).

**Effect of calcination temperature on activity of $TiO_2$ photocatalysts**

There were significant effects of calcination temperature on the photocatalytic activity in phenol decomposition (Figs.10a and 10b). At <700 °C, the

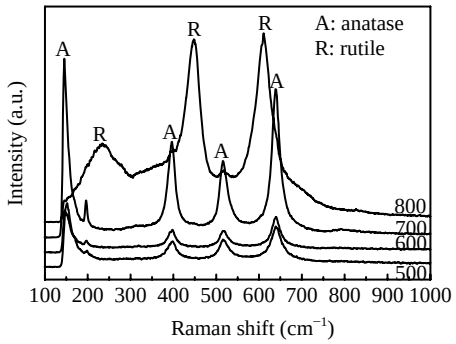


**Fig.9 Raman spectroscopy of catalysts**

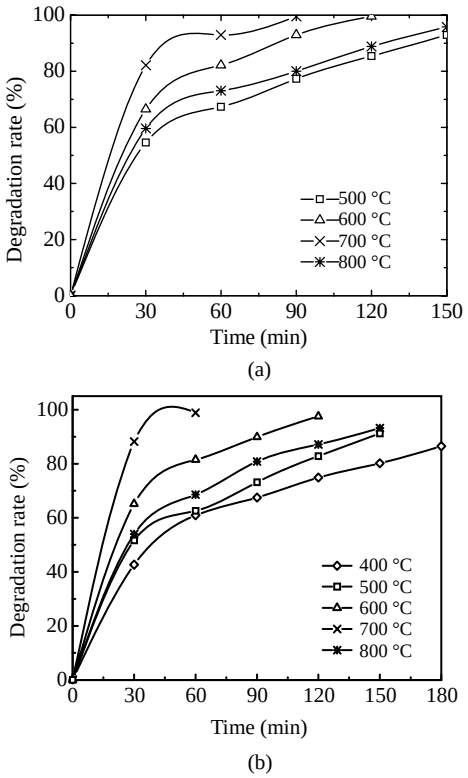


**Fig.10 Reactivity of TS(1:3) catalysts calcined at different temperatures (a) and TS(1:2) catalysts calcined at different temperatures (b)**

catalytic activity increased with increasing calcination temperatures and reached the highest at 700 °C, but at 800 °C the catalytic activity decreased. With calcination at 400 °C, the crystal form of TS(1:2) anatase was only partial and thus the catalytic activity was poor. After calcination at 500 °C and 600 °C, the anatase phase of catalysts steadily increased and their catalytic activity strengthened. With calcination at 700 °C, $SO_4^{2-}$ absorbed in $TiO_2$ precipitation began to decompose. According to Colon *et al.*(2006), $SO_4^{2-}$ decomposition can increase the $O^{2-}$ quantity on $TiO_2$ surface, which may prevent the recombination of electron-hole pairs and increase light efficiency of photocatalysts and photocatalytic activity. In this study, the crystal form of $TiO_2$ photocatalysts transformed to rutile rapidly (>70%), and as compared with the anatase surface, the catalytic centre of the rutile surface was much smaller and thus the activity of $TiO_2$ photocatalysts calcined at 800 °C decreased.

**Effect of $(NH_4)_2SO_4$ dosages on catalytic activity**

The degradation rate of catalysts prepared with $(NH_4)_2SO_4$ was >95% at a reaction time of less than 1.5 h, compared to 2.5 h for catalysts prepared without $(NH_4)_2SO_4$ (Fig.11). When the mole ratio of Ti:$(NH_4)_2SO_4$ was 1:2, the catalytic activity was the highest, with >99% degradation after 1 h reaction. At the mole ratios of 1:1, 1:3 and 1:4, the catalytic activities were very similar with the degradation rates of 95% after 1.5 h reaction. This was because when $(NH_4)_2SO_4$ dosage was small, the low concentration of $SO_4^{2-}$ decreased the absorption and activity of $TiO_2$. In contrast, a high $(NH_4)_2SO_4$ dosage caused the "hardening" phenomenon of $TiO_2$, which increased the particle size of $TiO_2$ precursors and thus increased the catalytic activity. The best $(NH_4)_2SO_4$ dosage was a mole ratio of Ti:$(NH_4)_2SO_4$=1:2, at which the degradation rate was >99% after 1 h reaction.

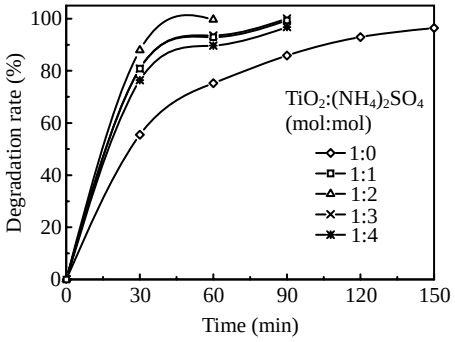


**Fig.11 Reactivity of catalysts with different dosages of $(NH_4)_2SO_4$**

**Effect of water-bath temperature on catalytic activity**

There was a big effect of water-bath temperature on catalytic activity (Fig.12). The activities of catalysts prepared at different water bath temperatures were in an order of 90 °C>70 °C>50 °C>30 °C. The particle size of catalysts prepared at 90 °C was the smallest (only 20 nm), followed by that at 70 °C (23 nm), at 50 °C (25 nm) and 30 °C (24 nm), whereas the specific surface area was in an order of 90 °C>70 °C>50 °C>30 °C (Table 2). According to the dimension effect of quantum (Ryoji *et al.*, 2006), particle-size diminution shortened the diffusion time of photo-electrons from the inner part to the outer surface of crystal and increased the effect of electron-hole separation. Meanwhile, the adsorption ability increased with augmenting specific surface areas and photocatalytic reactions. Namely, the activity of catalysts prepared at 90 °C was the highest.

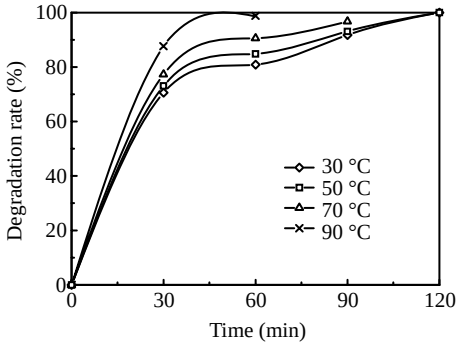


**Fig.12 Reactivity pattern of the catalysts prepared at different water bath temperatures**

**Effect of starting concentration of phenol on catalytic activity**

When dosages of TS(1:2)700 catalysts were the same, the starting concentration of phenol solution had a big effect on phenol degradation (Fig.13). The time of complete degradation increased with the increment of starting phenol concentrations. In addition, the activity of TS(1:2)700 catalysts was better with higher starting phenol concentrations. At a phenol concentration of 20 mg/L the complete degradation time was 1.5 h; at a phenol concentration of 40 mg/L the complete degradation time needed only 2 h.

Therefore, selecting a starting phenol concentration was important to examine catalytic activity.

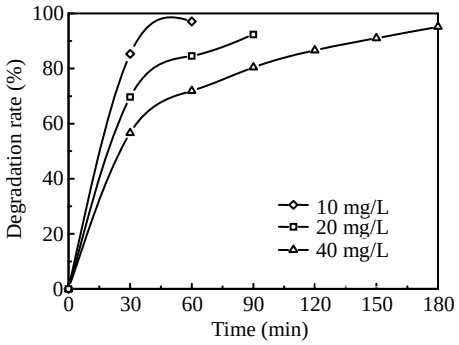


**Fig.13 Reactivity pattern of different start concentrations**

### Effect of catalyst dosage on catalytic activity

The rate of phenol degradation was also affected by catalyst dosage (Fig.14). With the same reaction time (1.5 h), the 0.2 g of catalyst dosage achieved 99.8% degradation, whereas 0.25 g and 0.15 g of catalysts achieved 95.1% and 93.7% degradation respectively. The effect was more significant if the catalyst dosage continued to increase or decrease: 85.1% degradation by 0.1 g catalyst; 87.7% degradation by 0.3 g catalyst. When the catalyst dosage was small there were few catalytic centers, but when the catalyst dosage exceeded a certain value, extra photocatalysts not only absorbed but also reflected and scattered UV light, reducing the sufficient use of UV light and thus phenol degradation (Choi *et al.*, 2005).

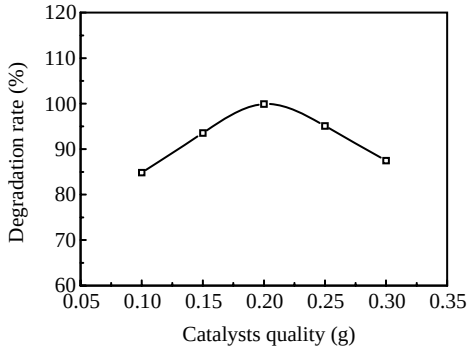


**Fig.14 Phenol decomposition at different catalyst dosages**

## CONCLUSION

(1) $TiO_2$ photocatalysts prepared by the hydrolyzation method with $(NH_4)_2SO_4$-modified $TiCl_4$ solution had big specific surface areas and small average particle sizes. At the water-bath temperature of 90 °C and the mole ratio of Ti:$(NH_4)_2SO_4$=1:2, photocatalysts calcined at 400 °C still had a specific surface area of 138.2 $m^2/g$ and an average particle size of 9 nm. At the calcination temperature of 700 °C, the specific surface area was 28.2 $m^2/g$ and the average particle size was 20 nm.

(2) High-temperature water-baths accelerated the precipitation of powdery $TiO_2$ and decreased the particle size of $TiO_2$, and also raised the uniformity of $TiO_2$ samples.

(3) $(NH_4)_2SO_4$ modifications improved the thermal stability of anatase phase. After calcination at 700 °C, crystal $TiO_2$ began to transform from anatase to rutile.

(4) Catalytic activity reached the highest at the mole ratio of Ti:$(NH_4)_2SO_4$=1:2, the water-bath temperature of 90 °C and the calcination temperature of 700 °C.

(5) TS(1:2)700 catalysts achieved 99.7% phenol degradation under the conditions: 10 mg/L of the starting phenol concentration, 2 g/L of the catalyst concentration, and 1 h of the irradiation by a 300 W high-voltage mercury lamp.

## References

Alemany, L.J., Banares, M.A., Pardo, E., 2000. Morphological and structural characterization of a titanium dioxide system. *Materials Characterization*, **44**(3):271-275. [doi:10.1016/S1044-5803(99)00066-2]

Choi, H.H., Park, J., Singh, R.K., 2005. Nanosized titania encapsulated silica particles using an aqueous $TiCl_4$ solution. *Applied Surface Science*, **240**(1-4):7-12. [doi:10.1016/j.apsusc.2004.06.147]

Colon, G., Hidalgo, M.C., Navio, J.A., 2003. Photocatalytic behaviour of sulphated $TiO_2$ for phenol degradation. *Applied Catalysis B: Environmental*, **45**(1):39-50. [doi:10.1016/S0926-3373(03)00125-5]

Colon, G., Hidalgo, M.C., Munuera, G., Ferino, I., Cutrufello, M.G., Navio, J.A., 2006. Structural and surface approach to the enhanced photocatalytic activity of sulfated $TiO_2$ photocatalyst. *Applied Catalysis B: Environmental*, **63**(1-2):45-59. [doi:10.1016/j.apcatb.2005.09.008]

Gao, L., Zhang, Q.H., 2001. The promoting effect of sulfate ions on the nucleation of $TiO_2$ (anatase) nanocrystals. *Materials Transactions*, **42**(8):1676-1680. [doi:10.2320/matertrans.42.1676]

Han, S.T., Xi, H.L., Shi, R.X., 2003. Prospect and progress in the semiconductor photocatalysis. *Chinese Journal of Chemical Physics*, **16**(5):339-349.

Jung, S.M., Grange, P., 2000. Characterization and reactivity

of pure $TiO_2$-$SO_4^{2-}$ SCR catalyst: influence of $SO_4^{2-}$ content. *Catalysis Today*, **59**(3-4):305-312. [doi:10.1016/S0920-5861(00)00296-0]

Mei, C.S., Zhong, S.H., 2004. Preparation and characterization of composite semiconductor photocatalyst Cu/$MoO_3$-$TiO_2$. *Chinese Journal of Catalysis*, **25**(11):862-868.

Ryoji, I., Takayuki, F., Masato, H., Teruhisa, O., 2006. Synthesis of nanosized $TiO_2$ particles in reverse micelle systems and their photocatalytic activity for degradation of toluene in gas phase. *Journal of Molecular Catalysis A: Chemical*, **260**(1-2):247-254. [doi:10.1016/j.molcata.2006.06.053]

Su, W.Y., Fu, X.Z., Wei, K.M., 2001. Effect of sulfation on structure and photocatalytic performance of $TiO_2$. *Acta Physico-Chimica Sinica*, **17**(1):28-31.

Ye, X.S., 2006. Preparation of iron hydroxide colloid. *Chemistry Education*, **27**(8):33-38.

Zhang, Q.H., Gao, L., Guo, J.K., 1999. Preparation and characterization of nanosized $TiO_2$ powders from aqueous $TiCl_4$ solution. *Nanostructured Materials*, **11**(8):1293-1300. [doi:10.1016/S0965-9773(99)00421-3]

Zhang, Q.H., Gao, L., Guo, J.K., 2000. Preparation of nanosized $TiO_2$ powders from hydrolysis of $TiCl_4$. *Journal of Inorganic Materials*, **15**:21-25.